The process $gg \to WW$ as a probe into the EWSB mechanism

E. Accomando[1]

[1]*INFN, Torino & Dipartimento di Fisica Teorica, Università di Torino, I-10125 Torino, Italy*

(Dated: September 3, 2007)

We present the first estimate of the gluon-gluon fusion process, gg $\to$ 4f, in the high energy domain as a probe of the electroweak symmetry breaking mechanism (EWSB). We consider the exact matrix element at $\mathcal{O}(\alpha_s\alpha_{em}^2)$, and we include all irreducible background coming from $q\bar{q} \to 4f$. Purely leptonic final states, $pp \to l\bar{\nu}_l\nu_{l'}\bar{l'}$, are numerically investigated. We find that this channel is extremely sensitive to the regime of the interaction between gauge bosons. It can thus be associated to the traditionally used vector boson scattering (VBS) to improve the analysis of the EWSB physics.

PACS numbers: 12.15.Ji, 14.70.Fm

The discovery of the EWSB physics will be the primary goal of the LHC. This Letter deals with the study of a new process, which could largely improve the LHC potential in this search. We consider the production of WW-pairs via gluon-gluon fusion, $gg \to WW \to 4f$. Usually analysed for the Higgs boson discovery, i.e. in the low-intermediate energy range where the Higgs resonance is expected to appear, this channel is here found to have a strong potential also at high energies. Our aim is to present the properties of the gluon-induced weak-boson pair production at the TeV scale, and to analyse their consequences on the phenomenology of the interaction between the produced gauge-bosons. The main motivation for such a study relies on the strict correlation between the regime of the gauge interaction and the mechanism which triggers the EWSB[1].

Many theories describe different EWSB scenarios. Most of them (Standard Model (SM), SUSY, etc.) predict the existence of at least one light Higgs. This hypotesis implies that the dynamics responsible of the spontaneous symmetry breaking is weakly-coupled. Such a picture is in good agreement with the LEP1 electroweak precision measurements. However, the Higgs is still missing. In addition, new theoretical developments have opened up the possibility to build new models of electroweak symmetry breaking (a recent review is given in Ref. [2]). They mainly fall into two classes. In the first case, the Higgs is still predicted but it is not an elementary particle. It is included as an effective field arising from a new dynamics which becomes strong at some energy scale (an example are the Little Higgs models). In the latter, the Higgs sector might even be completely replaced with strongly interacting dynamics. Interesting realizations of this scenario can arise in extra-dimensions theories.

Hence, in order to understand the nature of the new physics which will be discovered in the next future, a crucial issue to be settled is whether the EWSB dynamics is weakly or strongly coupled. A way of answering this question preserving a model independent approach is thus looking at processes involving at least one massive gauge-boson pair. Ideally, the vector boson scattering, $VV \to VV$ ($V = W, Z$), is the most sensitive process to the EWSB mechanism [1]. However, it is embedded in the more complex channel $q_1q_2 \to q_3q_4VV \to q_3q_4 + 4f$. Its sensitivity is thus depleted by limited number of events and huge backgrounds. For a recent and detailed status of VBS perspectives at the LHC see for instance Ref. [3] and references therein. The gluon-induced process can bring a powerful help in this challenge.

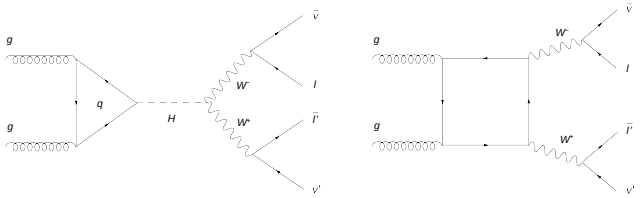

FIG. 1: Sample LO diagram for the gg $\to$ 4f process.

Let us begin with recalling that the leading-order (LO) contribution to the gluon-induced weak-boson pair production originates from one-loop diagrams in the SM. An example is shown in Fig. 1 [12]. The corresponding amplitudes were first evaluated in the on-shell vector-boson approximation, gg $\to$ VV [4, 5]. Successive computations took into account the spin correlations between gauge-boson production and decay, by considering the process gg $\to$ VV $\to$ 4f in narrow width approximation [6]. Recently, the first full calculation of the loop-induced W-boson pair production and decay, gg $\to$ 4leptons, was implemented in the code `gg2WW` and published [7]. It takes into account vector-boson off-shell effects, full spin and decay angle correlations, and the loop contribution coming from the massive third generation quarks.

Starting from this result, we have been able for the first time to perform a complete and realistic analysis of the gg $\to$ 4leptons process at high energies. Up to now, this channel has been considered only for Higgs boson discovery. Its behaviour has been thus analysed for kinematical configurations appropriate for the Higgs search, and at energy scales around the expected Higgs resonance. The new fit to the electroweak precision data has recently lowered the 95%C.L. bound on the Higgs mass down to about 144 GeV. If one takes this result as a reasonable indication, the scanned energy domain is quite narrow.

The purpose of this Letter is to extend the analysis at the TeV scale, and show that the gluon-fusion channel constitutes a powerful probe into the EWSB physics,

independently on the Higgs existence and discovery. Following a model-independent approach, we focus on the interaction between the produced weak-bosons. This interaction can be modified by the presence of new EWSB physics, which might appear at energy scales probed at the LHC or even larger. Having as a target the study of the sensitivity of the considered channel to possible new physics, we parametrize such a scenario by choosing the minimal realization, i.e. the Standard Model with no Higgs. And, we compare the outcoming results with the predictions of the SM with a light Higgs.

Our aim is to perform a complete and realistic analysis of the weak-boson pair production at the LHC, via the pp → 4leptons process (see e.g. Ref. [8] for a review on its present status). In addition to the gluon-induced signal, we have to consider the background coming from quark-induced contributions to the same final state, $q\bar{q} \to$ 4leptons. This background is overwhelming, but it can be heavily suppressed as shown later.

Before starting our analysis, let us summarize the numerical setup. In computing partonic cross-sections, for the SM free parameters we use the input values [9]:

$$\begin{aligned} M_{\rm W} &= 80.403\,{\rm GeV}, & M_{\rm Z} &= 91.1876\,{\rm GeV}, \\ m_{\rm t} &= 174.2\,{\rm GeV}, & m_{\rm b} &= 4.4\,{\rm GeV}, \\ G_\mu &= 1.16639\times 10^{-5}\,{\rm GeV}^{-2}. \end{aligned} \tag{1}$$

The weak mixing angle is fixed by $s^2_{\rm w} = 1 - M^2_{\rm W}/M^2_{\rm Z}$. We adopt the G_μ-scheme, which effectively includes higher-order contributions associated with the running of the electromagnetic coupling and the leading universal two-loop $m_{\rm t}$-dependent corrections. To this end we parametrize the LO matrix element in terms of the effective coupling $\alpha_{G_\mu} = \sqrt{2} G_\mu M^2_{\rm W} s^2_{\rm w}/\pi$. We moreover use the fixed-width scheme with $\Gamma_{\rm Z} = 2.44506\,{\rm GeV}$ and $\Gamma_{\rm W} = 2.04685\,{\rm GeV}$. As to parton distributions (PDF), we have chosen CTEQ6M [10] at the factorization scale $Q = M_{\rm W}$. We consider purely leptonic final states:

$$\mathrm{pp} \to \nu_{\rm l} {\rm l}^+ {\rm l'}^- \bar{\nu}_{\rm l'} \qquad {\rm l}, {\rm l'} = {\rm e}, \mu. \tag{2}$$

The signature is thus characterized by two isolated charged leptons plus missing energy. This channel includes the WW production as intermediate state. In the parton model, the corresponding cross sections are described by the following convolution

$$\begin{aligned} {\rm d}\sigma^{\rm pp}(P_1,P_2,p_f) = \int_0^1 {\rm d}x_1 {\rm d}x_2 \sum_{q={\rm g,u,d,c,s}} \Big[\Phi_{\bar{\rm q},{\rm p}}(x_1,Q^2) \\ \times \Phi_{{\rm q},{\rm p}}(x_2,Q^2)\, {\rm d}\hat{\sigma}^{\bar{\rm q}{\rm q}}(x_1P_1, x_2P_2, p_f) + \Phi_{\bar{\rm q},{\rm p}}(x_2,Q^2) \\ \times \Phi_{{\rm q},{\rm p}}(x_1,Q^2) \times {\rm d}\hat{\sigma}^{\bar{\rm q}{\rm q}}(x_2P_2, x_1P_1, p_f) \Big] \end{aligned} \tag{3}$$

where p_f summarizes the final-state momenta, Φ_{i,h_i} is the PDF of parton i in the incoming proton h_i with momenta P_i, and $\hat{\sigma}^{ij}$ represent the partonic, colour and spin avaraged, cross sections. The $\hat{\sigma}^{ij}$ are calculated at LO, using the matrix elements for the complete processes

$$\begin{aligned} g(p_1) + g(p_2) &\to f_3(p_3) + f_4(p_4) + f_5(p_5) + f_6(p_6) \\ \bar{q}_1(p_1) + q_2(p_2) &\to f_3(p_3) + f_4(p_4) + f_5(p_5) + f_6(p_6) \end{aligned} \tag{4}$$

where the arguments label the momenta p_i of the external gluons and fermions. This means that we include the full set of Feynman diagrams, in this way accounting for the resonant di-boson production as well as the irreducible background coming from non-doubly resonant contributions. Complete four-fermion phase spaces and exact kinematics are employed in our calculation.

$M^{\rm cut}_{\rm ll'}$	$\sigma_{\rm Box}(g_{1,2,3})/\sigma_{\rm Box}(g_{1,2})$	$\sigma_{H,{\rm Box}(g_3)}/[\sigma_H + \sigma_{{\rm Box}(g_3)}]$
0 GeV	1.16	0.57
500 GeV	5.35	0.09

TABLE I: Relative size of individual contributions to the process $\mathrm{pp} \to \nu_{\rm e} {\rm e}^+ \mu^- \bar{\nu}_\mu$ as a function of the cut on the invariant mass of the charged lepton pair. Table entries are explained in the text. Standard cuts are applied.

For the experimental identification of the final state particles, we have implemented a general set of cuts appropriate for the LHC, and defined as follows:

- lepton transverse momentum $P_{\rm T}({\rm l}^\pm) > 20\,{\rm GeV}$,
- missing transverse momentum $P^{\rm miss}_{\rm T} > 25\,{\rm GeV}$,
- charged lepton rapidity $|y_{\rm l}| < 2$, where $y_{\rm l} = -\log\left(\tan(\theta_{\rm l}/2)\right)$, and $\theta_{\rm l}$ is the polar angle of particle l (massless) with respect to the beam.

These are standard cuts, dedicated ones will be described at due time.

We begin our analysis by comparing the properties of the gluon-induced process in the low and high energy regime. An important difference is in the behavior of the top-bottom massive quark loop. At low energy, the contribution of the third quark generation to the box diagram is neglegible compared to the contribution of the first two generations. This behaviour changes drastically at high energies. The amplitude of the massive quark box grows with increasing energy, and becomes dominant. Moreover, it interferes strongly and destructively with the Higgs diagram. This is shown in Tab. I as a function of the cut on the invariant mass of the two charged leptons, $M^{\rm cut}_{\rm ll'}$. The second column presents the ratio between the full box cross section and the contribution of the first two generations. Whereas at low energies the top-bottom quark loop constitutes only the 16% of the total box cross-section, already for $M_{\rm ll'} > 500\,{\rm GeV}$ (which means $E_{\rm cm} \simeq 1\,{\rm TeV}$) it gets dominant by a factor 5 over the light quark generations. The third column shows instead the interference between the box graph mediated by the third generation quarks and the Higgs diagram. With increasing energy, the interference gets heavily negative and gives rise to a cancellation between the two amplitudes of about a factor 10.

Setup	$\sigma(q\bar{q})$ (fb)	$\sigma(gg)$ (fb)	$\sigma(q\bar{q})/\sigma(gg)$
no cuts	555.4	58.6	9.5
Standard cuts	128.2	24.1	5.3
Dedicated cuts	5.2	3.0	1.7

TABLE II: From left to right, SM $q\bar{q}$-background, gg-signal in the no-Higgs scenario, and their ratio for the process $pp \to \nu_e e^+ \mu^- \bar{\nu}_\mu$ and different sets of cuts, as described in the text.

An analogous feature is displayed by the loop-induced Z-boson pair production as discussed in Ref.[4]. This peculiar behaviour finds an explanation in the analitical expression of the matrix element. Both the Higgs and the massive quark box amplitudes squared exhibit indeed a logarithmic dependence on the center-of-mass energy of the $gg \to 4f$ process. Such an energy dependence can be interpreted as a relic of the much stronger energy dependence of the individual contributions to the on-shell process $t\bar{t} \to W^+W^- \to 4f$, obtained by cutting on the internal lines of the loops appearing in the graphs of Fig. 1 and related ones. The amplitude squared of the on-shell top-induced WW-pair production grows like $s = E^2_{\rm cm}$ in absence of the Higgs. The same energy dependence is shared by the additional Higgs contribution. Gauge and Higgs amplitudes interfere destructively in order to preserve the perturbative unitarity of the theory. This feature is not washed out by the convolution of the top-induced subprocess with the gluon-induced quark loop. A di-logarithmic energy dependence of the individual graphs indeed survives, as mentioned above.

We exploit this behaviour in order to quantify the sensitivity of the gluon-induced channel to possible new EWSB physics. We consider two benchmark scenarios: the SM with a light Higgs ($M_H = 120\,\text{GeV}$) and the SM with no Higgs (noH). For a realistic assessment of the potential of the considered process, one has to take into account the full background coming from the process $q\bar{q} \to 4$leptons and giving rise to the same final state. At first glance, this large contribution seems to bury away any possible new-physics signal. In absence of any cut, its cross section is a factor 10 bigger than the gluon-induced one. As shown in Tab. II, standard cuts help in reducing it down to a factor 5. But, still the discovery potential of the gluon-induced channel is largely spoiled. The only way to keep under control the large $q\bar{q}$-background is to exploit the pronounced differences shown in many variable distributions by this process compared to the loop-induced signal.

The most important kinematical difference is in the rapidity distribution of the final state leptons. The $q\bar{q}$-background tends to be produced at a larger rapidity, because of the harder distribution of the valence quarks. The second most important one lies in the spin state of the intermediate W-pair system. The signal we are interested in can be traced back to the production of longitudinal W-bosons, for it is this rate to be enhanced by possible new EWSB physics. Such a signal is expected to increase for high CM energies and large scattering angles

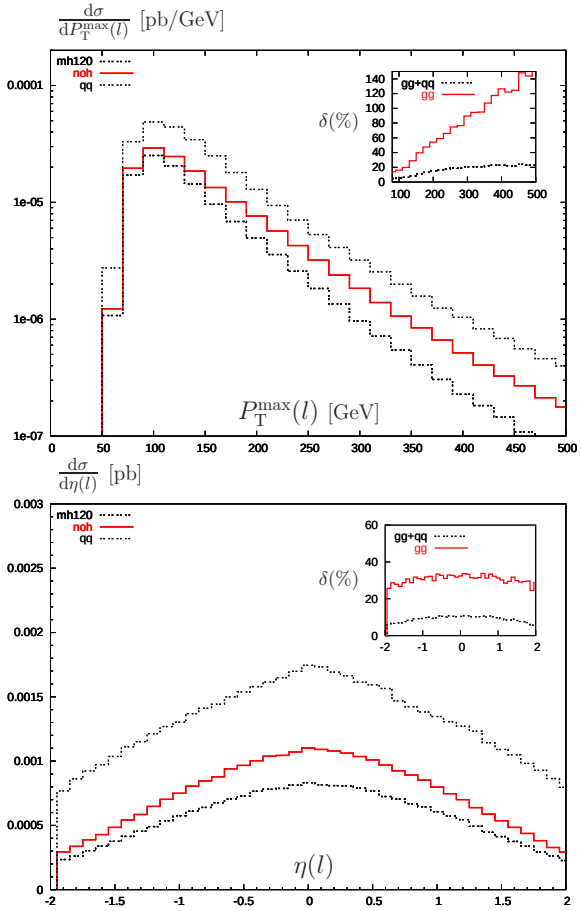

FIG. 2: a) Distribution in the maximal transverse momentum of the charged leptons. b) Distribution in the rapidity of the negatively charged lepton. We consider the process $pp \to \nu_e e^+ \mu^- \bar{\nu}_\mu$. From top to bottom, the three curves represent SM $q\bar{q}$-background, gg-signal with no Higgs, and gg-process in the SM ($M_H = 120\,\text{GeV}$). The inset plot gives the difference in percent between SM and noH scenarios for the gluon-induced (upper curve) and the full process (lower curve). Dedicated cuts are applied.

of the produced W's. In order to recover the lost sensitivity, we thus impose the following kinematical constraints:

- missing transverse momentum $P_T^{\rm miss} > 80\,\text{GeV}$,
- lepton azimutal angle difference $\Delta\phi(l^+l'^-) > 60^o$,
- charged lepton rapidity difference $\Delta y(ll') < 2$, where $\Delta y(ll') = |y_l - y_{l'}|$
- charged lepton opening-angle $\cos\theta(ll') > -0.98$.

With this choice, we refer to as dedicated cuts, the $q\bar{q}$-background becomes of the same order of magnitude as the gg-signal, as shown in the last row of Tab. II, partially recovering the lost sensitivity. The imposed cuts also select large energies ($E_{\rm cm} \geq 300\,\text{GeV}$) and angles, as of interest.

With these results at hand, we are ready to present the first estimate of the full $pp \to 4$leptons process at high energy scales. We call it estimate, because we do

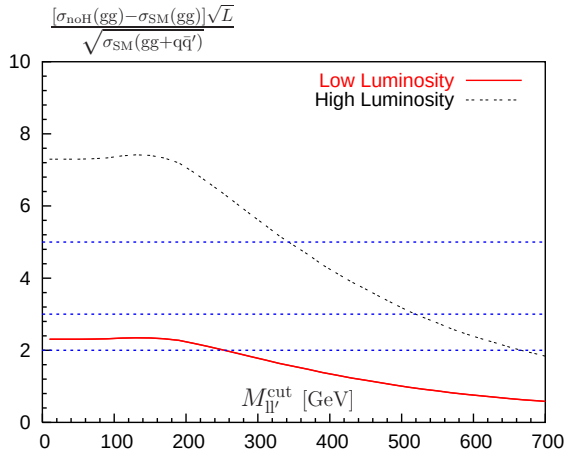

FIG. 3: Signal over background ratio, for the process $pp \to \nu_l l^+ l'^- \bar{\nu}_{l'}$. We sum over e and μ, and consider two luminosity values: $L = 10\,fb^{-1}$ (lower curve) and $L = 100\,fb^{-1}$ (upper curve). Dedicated cuts are applied.

$M_{ll'}^{cut}$ (GeV)	$N_{noH}(gg)$	$N_{SM}(gg)$	$N_{SM}(q\bar{q})$
0	751	572	1323
250	147	77	307
500	25	9	64

TABLE III: We consider the process $pp \to \nu_e e^+ \mu^- \bar{\nu}_\mu$. From left to right, number of events for gg-process with no Higgs, SM gg-process ($M_H = 120\,GeV$), and SM $q\bar{q}$-background for $L = 100\,fb^{-1}$. Dedicated cuts are applied.

not include NLO QCD corrections available for the $q\bar{q}$-background (see for instance Ref. [11]), but still missing for the gluon-induced signal. We show results for the LHC at $E_{cm} = 14\,TeV$. In Fig. 2, we plot two sample distributions in energy and angle, comparing the gluon-induced signal in the no-Higgs scenario (noH) with the SM prediction given by the $q\bar{q}$-background plus the gg-process with a light Higgs ($M_H = 120\,GeV$). The inset plots show that the difference between the two benchmark scenarios is enhanced at high energies and large angles of the outgoing charged leptons. Such a difference would be extremely pronounced if we considered only the gluon-fusion contribution, $\delta = \sigma_{noH}(gg)/\sigma_{SM}(gg) - 1$ (upper curves). The $q\bar{q}$-background reduces it, still preserving a difference, $\delta = \sigma_{noH}(gg)/\sigma_{SM}(gg + q\bar{q}) - 1$, up to 20% (lower curves).

In order to assess the sensitivity of the considered channel to possible new physics, one has to estimate the statistical significance of such effects. We naively derive it from their comparison with the statistical error expected at the LHC. In Fig. 3, we plot the signal over background ratio as a function of $M_{ll'}^{cut}$. We consider the two envisaged values of the luminosity, $L = 10\,fb^{-1}$ and $L = 100\,fb^{-1}$, corresponding to the low- and high-luminosity run. The three horizontal lines are the 2, 3 and 5 standard deviation reference values. Fig. 3 shows that at high luminosity, one can reach 2σ-effects and more over almost the entire energy range. Even in the low-luminosity run, one could explore sensitivity up to scales of the order of 500 GeV. The number of estimated events at high-luminosity is given in Tab. III as a function of $M_{ll'}^{cut}$.

To conclude, we have provided the first complete study of the $pp \to \nu_l l^+ l'^- \bar{\nu}_{l'}$ process at $\mathcal{O}(\alpha_s^2 \alpha_{em}^4)$ in the high energy domain. This channel is found to have strong potential for probing the nature of EWSB physics at the LHC. A final statement should include detector response and systematics; this goes beyond our purpose.

T. Binoth and M. Ciccolini are gratefully acknowledged for valuable discussions and their help in using the `gg2WW` code. This work was supported by MIUR under contract Decreto MIUR 26-01-2001 N.13 and contract $2006020509_0 04$, and by the European Community's MRTN under contract MRTN-CT-2006-035505.

[1] M.S. Chanowitz, hep-ph/9812215; S. Dawson, hep-ph/9901280; C. Quigg, Acta Phys. Polon. B **30**, 2145 (1999); S. Dawson, Int. J. Mod. Phys. A **21**, 1629 (2006).
[2] R. Rattazzi, PoS HEP2005:399,2006.
[3] E. Accomando, A. Ballestrero, A. Belhouari, E. Maina, Phys. Rev. D **75**, 113006 (2007); E. Accomando, A. Ballestrero, S. Bolognesi, E. Maina, C. Mariotti, JHEP 0603:093,2006; E. Accomando, A. Ballestrero, E. Maina, JHEP 0507:016,2005; E. Accomando, A. Ballestrero, E. Maina, Nucl. Instrum. Meth. A **534**, 265 (2004); N.Amapane et al, CMS AN 2007/005.
[4] E.W.Nigel Glover, J.J. van der Bij, Phys. Lett. B **219**, 488 (1989); E.W.Nigel Glover, J.J. van der Bij, Nucl. Phys. B **321**, 561 (1989).
[5] C. Kao, D.A. Dicus, Phys. Rev. D **43**, 1555 (1991).
[6] M. Duhrssen, K. Jakobs, J.J. van der Bij, P. Marquard, JHEP 0505:064, 2005; T. Matsuura, J.J. van der Bij, Z. Phys. C **51**, 259 (1991); C. Zecher, T. Matsuura, J.J. van der Bij, Z. Phys. C **64**, 219 (1994).
[7] T. Binoth, M. Ciccolini, N. Kauer, M. Kramer, JHEP 0612:046, 2006; T. Binoth, M. Ciccolini, N. Kauer, M. Kramer, JHEP 0503:065, 2005.
[8] S. Haywood *et al.*, hep-ph/0003275, in *Standard Model Physics (and more) at the LHC*, eds. G. Altarelli and M. L. Mangano, (CERN-2000-004, Genève, 2000) p. 117.
[9] K. Hagiwara *et al.* [Particle Data Group Collaboration], Phys. Rev. D **66** (2002) 010001; The CDF Collaboration, the D0 Collaboration, the Tevatron Electroweak Working Group, hep-ex/0404010.
[10] J. Pumplin, D.R. Stump, J. Huston, H.L. Lai, P. Nadolsky and W.K. Tung, JHEP 0207 (2002) 012.
[11] J. Ohnemus, Phys. Rev. D **44** (1991) 1403; S. Frixione, Nucl. Phys. B **410**, 280 (1993); J. Ohnemus, Phys. Rev. D **50** (1994) 1931; L.J. Dixon, Z. Kunszt, A. Signer, Nucl. Phys. B **531**, 3 (1998); L.J. Dixon, Z. Kunszt, A. Signer, Phys. Rev. D **60** (1999) 1140.
[12] For massless external particles, diagrams in Fig. 1 are the

only ones to contribute owing to the Furry's theorem.